The Farthest Point Map on the Regular Octahedron

Richard Evan Schwartz *

January 7, 2021

1 Introduction

1.1 Background

A classic recreational problem in mathematics poses the following kind of question: Given a point on the surface of box, what is the farthest point away in the intrinsic sense? The *intrinsic sense* means that distances between points on the surface are measured in terms of lengths of paths on the surface of the box and not in terms of the ambient 3-dimensional Euclidean distance. The solution to this problem usually involves unfolding the surface and pressing it into the plane, so that the shortest paths can be studied in terms of ordinary planar geometry. In this paper we will study the same kind of question for the surface of the regular octahedron.

We begin with some generalities. Let (X, d) be a compact metric space. The *farthest point map*, or *farpoint map* for short, associates to each point $p \in X$ the set $F_p \subset X$ of points $q \in X$ which maximize the distance function $q \to d_X(p, q)$. From a dynamics point of view, it is nicer to have a map from points of X to points of X rather than from points of X to subsets of X. So, let $X' \subset X$ be the set of points $p \in X$ such that F_p is just a single point. We then have a well defined map $F : X' \to X$, which carries p to the unique point in X farthest from p. To get a dynamical system, we define $X^{(1)} = X'$. Inductively we let $X^{(n+1)}$ be the set of those points $p \in X'$ such

*Supported by N.S.F. Grant DMS-1807320

that $F(p) \in X^{(n)}$. The full orbit is well defined on

$$X^{(\infty)} = \bigcap_{n=1}^{\infty} X^{(n)}. \tag{1}$$

In nice cases, $X^{(\infty)}$ is large enough to still be interesting.

I learned about the farpoint map on the regular octahedron from Peter Doyle, whose undergraduate student Annie Laurie Muahs-Pugh studied it in her Dartmouth College undergraduate thesis. At some point I wrote a graphical user interface, called *Spider's Embrace* [**S1**], which revealed essentially all the structure. In the intervening years, my PhD student Zili Wang wrote a thesis and a subsequent paper [**W**] which took Spider's Embrace as inspiration. She generalized some of the results to the case of centrally symmetric octahedra having all equal cone angles. I thought it would be good to rigorously prove the things I discovered using Spider's Embrace.

This paper has some overlap with other papers on the farpoint map. J. Rouyer's paper [**R1**] uses methods similar to the one in this paper to give an explicit computation of the farthest point map on the regular tetrahedron. The papers [**R2**], [**R3**] study the farthest point map for general convex polyhedra, and (as we point out later in the paper) contain more general versions of a few of our subsidiary lemmas. The papers [**V1**], [**V2**], [**VZ**], and [**Z**] study the map on general convex surfaces. One focus has been on Steinhaus's conjecture concerning the ubiquity of points p such that F_p is a single point.

1.2 Statement of Results

Henceforth X denotes the regular octahedron equipped with its intrinsic surface metric. Rather than think about the map F, it is nicer to think about the composition

$$f = FA = AF, \tag{2}$$

where $A : X \to X$ is the antipodal map. As our notation suggests, A and F commute. At first it might appear that in fact $A = F$, so that f is the identity map, but this is not the case. Note that $f^2 = F^2$, so we are not really changing the problem much by studying f instead of F.

The map f commutes with every isometry of X, so it suffices to describe the action of f on a fundamental domain for the action of the isometry group. One sixth of a face of X serves as such a fundamental domain. After suitably scaling the metric and taking local coordinates, we can take for a fundamental domain the triangle T having vertices

$$0, \qquad 1, \qquad \left(\frac{1}{4}, \frac{\sqrt{3}}{4}\right) \tag{3}$$

Figure 1.1 shows a picture of T and an auxiliary curve J. Figure 1.2 below shows how T sits inside the (orange) face of X containing it.

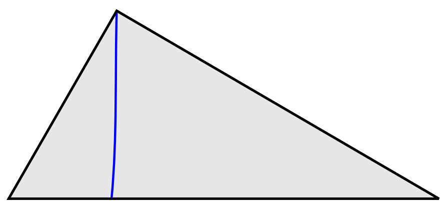

Figure 1.1: The domain T and the curve J.

The curve J is the graph of the function

$$y = \frac{1}{\sqrt{3}}\left(1 - x - ((2+x)(5-2x)(1-4x))^{1/3}\right), \tag{4}$$

on the interval $[r, 1/4)$. Here $r \approx .239123$ is the real root of $x^3 - x^2 - 4x + 1$. We do not consider the top endpoint to be belong to J.

Theorem 1.1 (Main) *If $p = (x + iy) \in T - J$ then F_p is a single point. If $p \in T - J$ lies to the left of J, then*

$$f(p) = \left(\frac{-xy - \sqrt{3}x + \sqrt{3}y^2 - y}{\sqrt{3}x + y - 2\sqrt{3}}, y\right) = \left(\frac{A_y x + B_y}{C_y x + D_y}, y\right). \tag{5}$$

if $p \in J$ lies to the right of J, then

$$f(p) = \left(\frac{-xy + 2\sqrt{3}x + \sqrt{3}y^2 - y}{\sqrt{3}x + y + \sqrt{3}}, y\right) = \left(\frac{D_y x - B_y}{-C_y x + A_y}, y\right). \tag{6}$$

If p is the top vertex of T then $f(p) = p$. If $p \in J$ then F_p is the union of the two points given by the formulas above.

Figure 1.2 shows a geometric interpretation of the Main Theorem. The blue triangle is the fundamental domain T and the orange triangle corresponds to the face of X containing T. The grey triangle is a reflected copy of the orange one. The map in Equation 5 maps the blue point to the white point (on the same horizontal line) and the map in Equation 6 maps the white point to the blue point. In particular, the two branches of f in T, when analytically continued to have a common domain, are inverses.

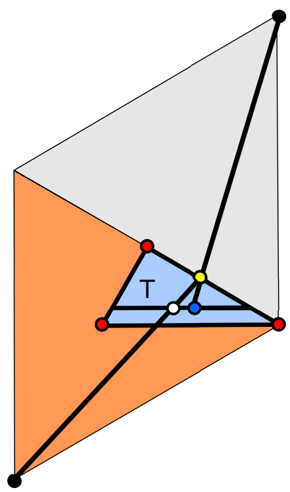

Figure 1.2 Geometric view of the maps.

Let $L_\infty(f)$ denote the ω-*limit set*. A point p belongs to $L_\infty(f)$ is there is some point q such that $\lim_{n\to\infty} f^n(q) = p$. We can use our result above to find $L_\infty(f)$ precisely. The restriction of f to each maximal horizontal line segment λ of $T - J$ is a linear fractional transformation having a unique fixed point in λ. The fixed point, namely $\lambda \cap \partial T$, is attracting. This fact, together with the rest of the Main Theorem, gives us the following corollary.

Corollary 1.2 *Let $\partial_\infty T$ denote the union of the non-horizontal sides of T.*

1. $X' \cap T = X^{(\infty)} \cap T = T - J$.
2. *Let $p \in T - J$. Then $f(p) = p$ if and only if $p \in \partial_\infty(T)$.*
3. $L_\infty(f) \cap T = \partial_\infty T$.

Figure 1.3 shows the intersection of $L_\infty(f)$ with one face of X.

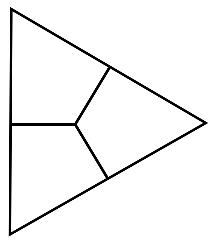

Figure 1.3: $L_\infty(f)$ in one face.

Figure 1.4 shows the image of the set J under 10 iterates of the dynamics. This picture illustrates how the dynamics moves points near J out to the boundary of T. Let J_ℓ and J_r be two copies of J which, so to speak, lie infinitesimally to the left and the right of J. We will iterate the left branch of f on J_ℓ and the right branch on J_r. We have shaded in the regions between $f^k(J_\ell)$ and $f^k(J_r)$ for $k = 1, ..., 10$.

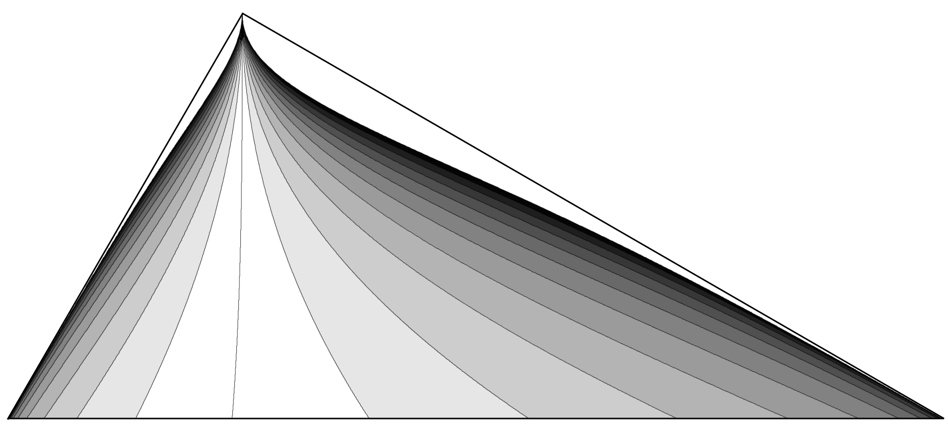

Figure 1.4: Iterates of J under the dynamics.

In §2 we prove the Main Theorem modulo some details we take care of in §3 and §4.

1.3 Acknowledgements

I thank Peter Doyle, Annie Laurie Mauhs-Pugh, and Zili Wang for interesting discussions about this question. I thank the anonymous referee for many helpful comments and suggestions. I thank the Simons Foundation for their support, in the form of a 2020-21 Simons Sabbatical Fellowship. Finally, I think the Institute for Advanced Study for their support, in the form of a 2020-21 membership funded by a grant from the Ambrose Monell Foundation.

2 The Proof in Broad Strokes

2.1 The Octahedral Plan

As in the introduction, X denotes the regular octahedron equipped with its intrinsic metric. X is locally Euclidean except for 6 cone points, each having cone angle $4\pi/3$. As a polyhedron, X has 8 *faces*, each an equilateral triangle. Let T be the fundamental domain discussed in the introduction. The blue triangle in Figure 2.1 is T. The black vertex of T, which we call the *sharp vertex*, corresponds to a cone point of X. Let Δ_0 denote the face of X that contains T. We identify Δ_0 with the triangle in the plane whose vertices are the cube roots of unity. The face Δ_0 is the one labeled 0 in Figure 2.1.

We call the equilateral triangles of P *faces*. By convention, a face is closed. There is a (unique) continuous locally isometric surjective map

$$\Psi : P \to X \tag{7}$$

which is the identity on Δ_0. We picture X as sitting on Δ_0, and Ψ wraps P around X as if we were wrapping a gift. We have numbered the faces of P to indicate their images under Ψ. The map Ψ carries the faces labeled 7 to the face of X antipodal to Δ_0. Let A_k be the 7-face also labeled (k). Finally, we mention that the blue circle, centered on the sharp vertex, has radius 3.

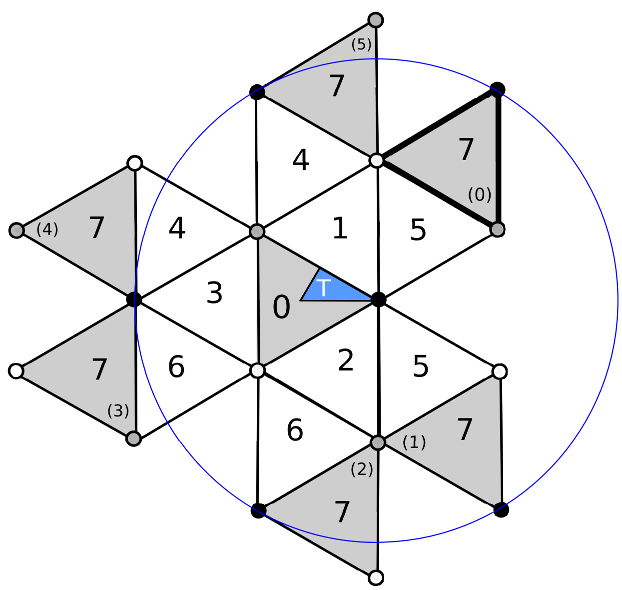

Figure 2.1: The octahedral plan P.

The 6 cone points of X are grouped into 3 pairs of antipodal points. We use 3 colors to color these pairs: black, white, and grey. The vertices of the octahedral plan are colored according to this scheme. Thus, Ψ maps all the white vertices to the union of the two white cone points of X, and likewise for the other colors. The next result is contained in [**R3**, Corollary 13]. We give a self-contained proof.

Lemma 2.1 *If p is a cone point then F_p is just the antipodal point.*

Proof: It suffices to prove this when p is the sharp vertex of T. Let p' be the antipodal point. Rolling X out onto the equilateral tiling along a shortest geodesic segment connecting p to p', we see that the image of p' is another black vertex of the planar tiling. The closest black vertices to p lie on (the blue circle) ∂D, where D is the disk of radius 3 centered at p. Hence $d_X(p,p') = 3$. Looking at Figure 2.1, we see that D^o contains all points of a j-face, except perhaps the black vertex, for each $j = 0,...,7$. Hence $\Psi(D^o) = X - p'$. Hence, $d_X(p,q^*) < 3$ for all $q^* \in X - p'$. ♠

We prove the following result in §3.

Lemma 2.2 (Octahedral Plan) *If $p \neq q^* \in X$, with $p \in \Delta_0$ not a cone point, then we have $d_X(p,q^*) = |p-q|$ for some $q \in \Psi^{-1}(q^*)$. If $q^* \in F_p$, the point q lies in a 7-face of P.*

The Octahedral Plan Lemma combines with the properties of Ψ to give the following more precise result: As long as $\Psi^{-1}(q^*)$ contains a point in a 7-face, we have

$$\Psi^{-1}(q^*) = \{q_0,...,q_5\}, \qquad \forall j \ q_j \in A_j, \qquad d_X(p,q^*) = \min_k |p-q_k|. \tag{8}$$

2.2 The Hexagon

Let T^o be the interior of the fundamental domain T. There are (unique) isometries I_j for $j = 0,...,5$ such that:

- I_j preserves the white-black-grey vertex coloring.
- $I_j(A_j) = A_0$.
- $\Psi \circ I_j = \Psi$ on A_j and $\Psi = \Psi \circ I_j^{-1}$ on A_0.

Referring to the points in Equation 8, these properties imply that

$$I_j(q_j) = I_k(q_k), \qquad \forall j,k \in \{0,....,5\}. \tag{9}$$

For a proof, use the fact that $\Psi : A_0 \to X$ is injective.

The map I_0 is the identity. If $j \equiv i+3$ mod 6 then $T_iT_j^{-1}$ is a translation. Otherwise $T_iT_j^{-1}$ is a 120 degree rotation about a vertex v_{ij}. These are the big colored vertices in Figure 2.4 below. We let $T_j = I_j(T)$. The blue triangles in Figures 2.2 are $T_0, ..., T_5$. Given $p \in T$ (not the sharp vertex) we define

$$p_j = I_j(p) \in T_j, \qquad j = 0, ..., 5. \tag{10}$$

Let H_p be the (solid) hexagon with vertices $p_0, ..., p_5$.

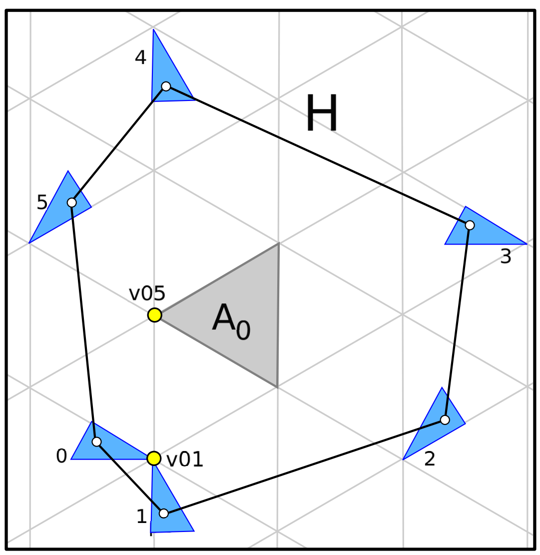

Figure 2.2: The hexagon H_p and the triangle A_0.

Lemma 2.3 *H_p is strictly convex.*

Proof: Given the placement of the blue triangles, it is clear that H_p is locally convex at p_j for $j = 1,2,3,4,5$. Consider the case $j = 0$. Clockwise rotation by 120 degrees about v_{01} maps p_1 to p_0. Clockwise rotation by 120 degrees about v_{05} maps p_0 to p_5. From this property we see that $\overline{p_0p_1}$ has slope in $[-\sqrt{3}, 0)$ and $\overline{p_0p_5}$ has slope in $[-\infty, -\sqrt{3})$. This shows that H_p is locally convex at p_0. ♠

2.3 The Voronoi Decomposition

Given $q \in H_p$ let

$$\mu_p(q) = \min_{k \in \{0,...,5\}} |q - p_k|. \tag{11}$$

We say that a *minimal index for* q is an index j such that $\mu_p(q) = |q - p_j|$. The jth *Voronoi cell* C_j is the set of points $q \in H_p$ having j as one of their minimal indices. That is, $\mu_p(q) = |q - p_j|$. The list $C_0, ..., C_5$ is the *Voronoi decomposition* of H_p. The Voronoi cells are convex polygons. Their edges are contained in the union of bisectors defined by pairs of vertices of H_p. See Figures 2.3 and 2.4

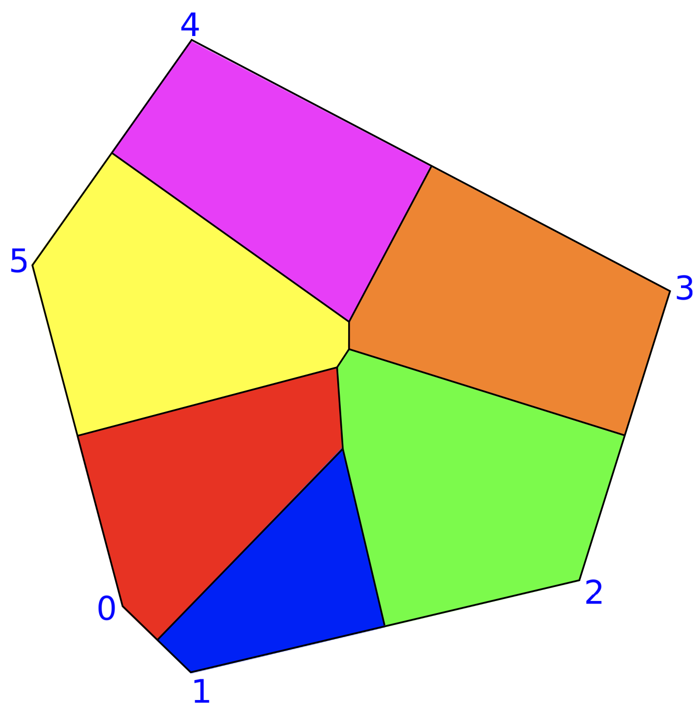

Figure 2.3: H_p and its Voronoi decomposition.

Remark: I produced Figure 2.3 in Mathematica, using the same formulas I use in §4 to do the calculations in the paper. The picture corresponds to the parameters $a = b = 1/2$. I mention this as a sanity check that I have correctly typed the formulas in to Mathematica. Figure 2.4 and 2.5 are produced by my Java program.

Given distinct indices i, j, k, let (ijk) as the unique point equidistant from vertices p_i, p_j, p_k. Lemma 2.3 guarantees that this point is well-defined and various continuously with $p \in T$. Relatedly, we say that an *essential vertex* is a point belonging to at least 3 Voronoi cells. In Figure 2.3 there are 4 distinct essential vertices, namely: $(012), (025), (235), (345)$. In §4 we prove:

Lemma 2.4 (Structural Stability) *For all $p \in T$ the essential vertices are (012), (025), (235), (345). When $p \in T^o$ these 4 triples are distinct.*

In the boundary case the 4 triples are never (completely) distinct. See Figure 2.5 below for an example. If $(012) = (235)$ we write (0235), etc.

Let T' denote the edge of T that lies in the edges of the equilateral tiling. This is the long non-horizontal side. See Figure 2.4. Also, Figure 2.5 shows why we need to exclude T' in our next result.

Lemma 2.5 *If $p \in T - T'$ then (012), (025), (235), (345) lie in A_0^o.*

Proof: Our proof refers to Figure 2.4 below. We will repeatedly use the properties of the maps $T_i T_j^{-1}$ discussed above. We get our various bounds by considering the actions of these maps (usually 120 degree rotations) on the extreme points in T_j. Let $\overleftrightarrow{e}$ denote the line extending the edge e.

We have $v_{45} \in b_{45}$, and b_{45} lies between $\overline{v_{45}v_{34}}$ and $\overline{v_{45}v_{12}}$, and $v_{34} \not\in b_{45}$. Hence b_{45} intersects both edges e_{23} and e_{45}, and not at the vertex v_{34}. At the same time, $v_{34} \in b_{34}$, and b_{34} lies strictly between $\overleftrightarrow{e_{23}}$ and $\overleftrightarrow{e_{45}}$. Hence $(345) = b_{45} \cap b_{34} \in A_0^o$. The proof for (012) is the same, with indices $0, 1, 2$ in place of $5, 4, 3$.

Since $v_{35}, (345), (235)$ are collinear, and $v_{02}, (012), (025)$ are collinear, and $v_{35}, v_{34}, v_{12}, v_{02}$ are collinear, and $(012), (235) \in A_0^o$ we see that (235) and (025) lie to the left of $\overleftrightarrow{e_{23}}$. The altitude of A_0 through v_{34} is parallel to b_{25} and either equals b_{25} (in an extreme case) or lies to the left of it. Hence (025) and (235) lie to the right of $\overleftrightarrow{e_{45}}$. Since $v_{05} \in b_{05}$ lies to the right of b_{25} and has non-negative slope, (025) lies above $\overrightarrow{e_{01}}$. Since $v_{23} \in b_{23}$ lies to the left of b_{25} and has non-positive slope, we see that (235) lies above $\overrightarrow{e_{01}}$. ♠

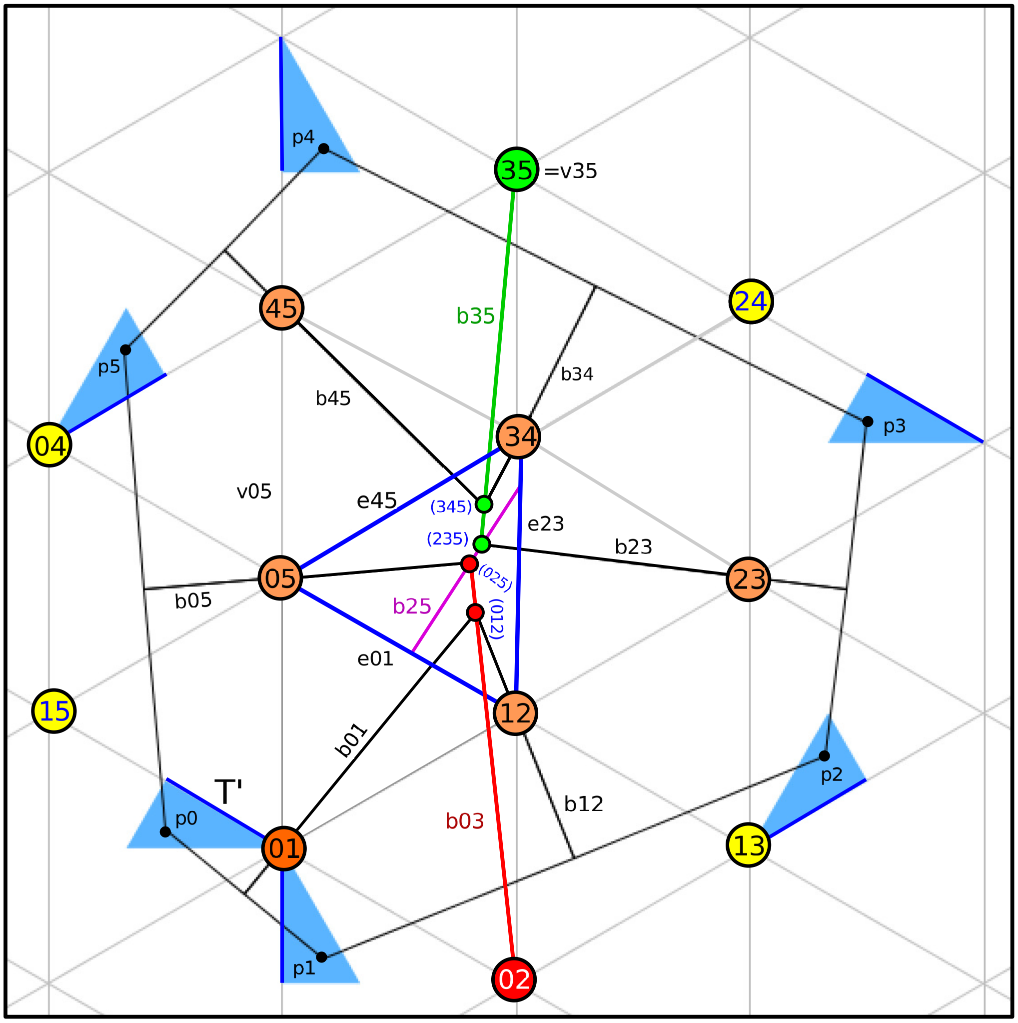

Figure 2.4: H_p and its Voronoi decomposition.

Lemma 2.5 combines with the Structural Stability Lemma to show that the essential vertices lie in A_0 even when $p \in \partial T$. The only case not covered by what we have already done is when $p \in T'$. When $p \in T'$, reflection in e_{23} swaps p_0, p_5 with p_2, p_3. This gives us $(345) = v_{34}$ and $(012) = v_{12}$ and $(025) = (235) \in e_{23}^o \subset b_{02} = b_{35}$. We get $(0235) \in e_{23}^o$ because we are excluding the sharp point. See Figure 2.5. We also note that $(025) = (235)$ when p lies in the short non-horizontal edge of A_0. In this case, reflection in the horizontal line through v_{05} swaps p_0, p_2 with p_5, p_3.

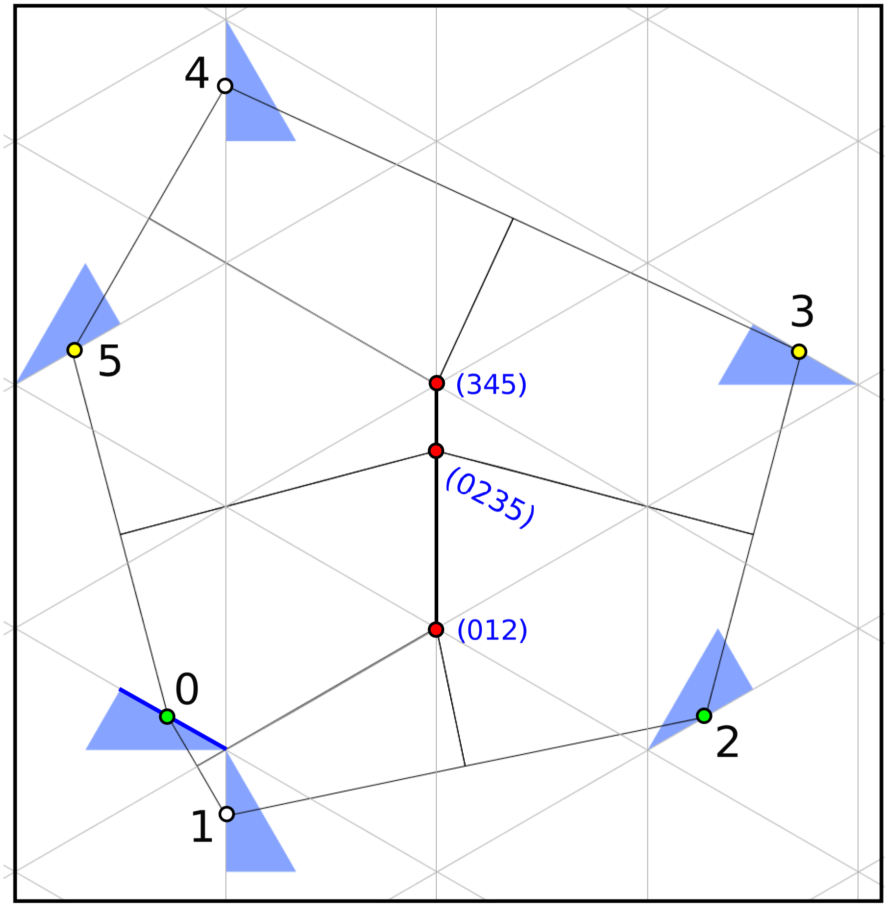

Figure 2.5: H_p and its Voronoi decomposition.

Lemma 2.6 *Let $q \in A_0$. If q is not an essential vertex then there is some $r \in A_0$ such that $\mu_p(q) < \mu_p(r)$.*

Proof: If q is disjoint from all cells but at most 2, we have at least one direction where we can vary q so as to increase μ_p. If $q \in A_0^o$ we are done. If $q \in \partial A_0$ and lies in only one cell, then q cannot be a vertex of A_0, so we can vary q in at least one direction along the edge of ∂A_0 so as to increase μ_p. This leaves the case when $q \in \partial A_0$ lies $C_i \cap C_j$. Since all essential vertices lie in A_0, the bisector b_{ij} starts out on ∂H_p, enters A_0, then encounters an essential vertex β before exiting A_0. After b_{ij} hits β it is disjoint from C_i and C_k. Therefore, q lies between $b_{ij} \cap \partial H_p$ and β. But then we push q along b towards β to increase μ_p, and this keeps us in A_0. ♠

2.4 Setting up a Vertex Competition

The reader can compare our next result with [**R2**, Lemma 3]. The result there, though stated in different language, is essentially equivalent.

Lemma 2.7 (Vertex) *If $q^* \in F_p$, then $q^* = \Psi(q)$ where $q \in A_0$ is such that $\mu_p(q) \geq \mu_q(r)$ for all $r \in A_0$. In particular, q is an essential vertex.*

Proof: Let $q_0, ..., q_5$ be as in Equation 8. Let $q = q_0$. By Equations 8 and 9, we have

$$q = I_0(q_0) = ... = I_5(q_5) \in A_0, \qquad \Psi(q) = q^*.$$

Since I_j is an isometry, $|p - q_k| = |p_k - q|$ for all k. Hence

$$d_X(p, q^*) = \min_k |q_k - p| = \min_k |q - p_k| = \mu_p(q). \tag{12}$$

For any $r \in A_0$ we set $r^* = \Psi(r)$. Then Equation 8 applies to r^* just as to q^*. Hence, Equation 12 holds as well. This gives

$$\mu_p(r) = d_X(p, r^*) \leq d_X(p, q^*) = \mu_p(q).$$

In short $\mu_p(q) \geq \mu_p(r)$ for all $r \in A_0$. By Lemma 2.6, the point q is an essential vertex. ♠

Lemma 2.8 $F_p \subset \{\Psi((025), \Psi((235))\}$.

Proof: Our argument refers to Figure 2.4. The Structural Stability Lemma and the Vertex Lemma imply that

$$F_p \subset \{\Psi((012)), \Psi((025), \Psi((235)), \Psi((345))\},$$

The line $\overleftrightarrow{p_0p_2}$ lies entirely beneath A_0 and in particular beneath the segment of b_{02} connecting (012) to (025). Also, $\overleftrightarrow{p_0p_2}$ and b_{02} are perpendicular. Therefore, as we move from $\zeta = (012)$ to $\zeta = (025)$ along b_{02} we increase the function $|\zeta - p_0| = |\zeta - p_2|$. This shows that $\mu_p((012)) < \mu_p((025))$ whenever $(012) \neq (025)$. The Vertex Lemma now eliminates (012) when it does not equal (025).

Since p is not the sharp vertex, the same argument, with the indices $5, 4, 3, 2$ in place of $0, 1, 2, 3$, shows that $\mu_p((345)) < \mu_p((235))$ whenever $(345) \neq (235)$. The Vertex Lemma now eliminates (345) when it does not equal (235). ♠

2.5 The Vertex Competition

Let

$$G(p) = |p_2 - (025)|^2 - |p_2 - (235)|^2. \tag{13}$$

In §4.2, we show that

- $G(p) > 0$ if $p \in T - \partial_\infty(T)$ lies to the left of J.
- $G(p) < 0$ if $p \in T - \partial_\infty(T)$ lies to the right of J.
- $G(p) = 0$ on $J \cup \partial_\infty T$.

By the Vertex Lemma and Lemma 2.8,

- $F_p = \Psi((025))$ when $p \in T - \partial_\infty T$ lies to the left of J and
- $F_p = \Psi((235))$ when $p \in T - \partial_\infty T$ lies to the right of J.
- $F_p = \{\Psi((025), \Psi((235))\}$ when $p \in J \cup \partial_\infty T$.

The last case needs more analysis. When $p \in \partial_\infty(T)$ we have $(025) = (235)$, as already discussed. When $p \in J$, the points (025) and (235) are distinct. The Structural Stability Lemma shows this for points of $J \cap T^o$. For the bottom endpoint of J, see the remark at the end of §4.1.

It only remains to get the formulas from the Main Theorem. Recall that $f = FA = AF$ where A is the antipodal map and F is the farpoint map. Define

$$\alpha_0(z) = \exp^{-2\pi i/3}(2 - i\sqrt{3} - \overline{z}). \tag{14}$$

The map α_0 has the propery that $\alpha_0(A_0) = \Delta_0$, in a way that preserves the vertex coloring in Figure 2.1. Hence

$$\Psi \circ \alpha_0 = A \circ \Psi.$$

So, when $F_p = \Psi((025))$, we get $f(p) = \alpha_0((025))$. This is exactly the map given in Equation 5. When $F_p = \Psi((235))$, we get $f(p) = \alpha_0((235))$. This is exactly the map given in Equation 5. Finally, when $p \in \partial_\infty(T)$, either formula gives $f(p) = p$. This establishes all parts of the Main Theorem.

3 The Octahedral Plan Lemma

3.1 General Points

In this section we prove the first statement of the Octahedral Plan Lemma.

Lemma 3.1 *If $p \neq q^* \in X$, with $p \in \Delta_0$ not a cone point, then we have $d_X(p, q^*) = |p - q|$ for some $q \in \Psi^{-1}(q^*)$.*

Proof: Let α^* be a length-minimizing geodesic segment connecting p to q^*. Since p is not a cone point, and since X has positive curvature at the other cone points, α^* contains no cone points in its interior. We can therefore uniquely develop X out onto the equilateral tiling, along α^*, to get a segment $\alpha \subset \boldsymbol{R}^2$. The segments α and α^* have the same length. Since P is star shaped with respect to p, we have $\Psi(q) = q^*$ provided that $q \in P$. We will suppose $q \notin P$ and get a contradicton.

By symmetry it suffices to consider the case when α crosses the two blue edges in Figure 3.1. If α exits P then it exits through one of the red edges. So, by passing to a sub-arc of α^*, which is also a distance minimizer, we can assume without loss of generality that q lies in either the yellow face or one of the green faces.

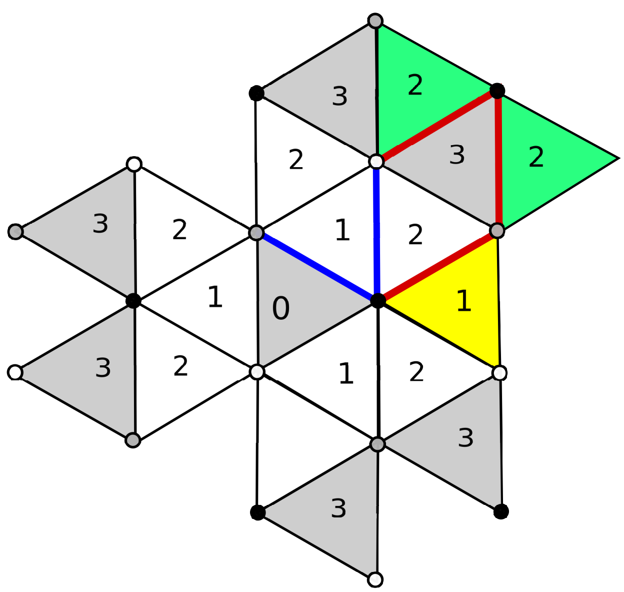

Figure 3.1: Filling in around the octahedral plan

We have relabeled the faces of P so that the face ζ is labeled according to the combinatorial distance from $\Psi(\zeta)$ to Δ_0. The colored faces do not belong to P, but nonetheless we can give them numerical labels. If q lies in one of the yellow faces then q^* must lie in a face which has combinatorial distance 1 from Δ_0 because this face shares a vertex with Δ_0 and cannot have the same label as an adjacent face. The green faces have label 2 because a subarc of α connects p to a point in the adjacent face labeled 3.

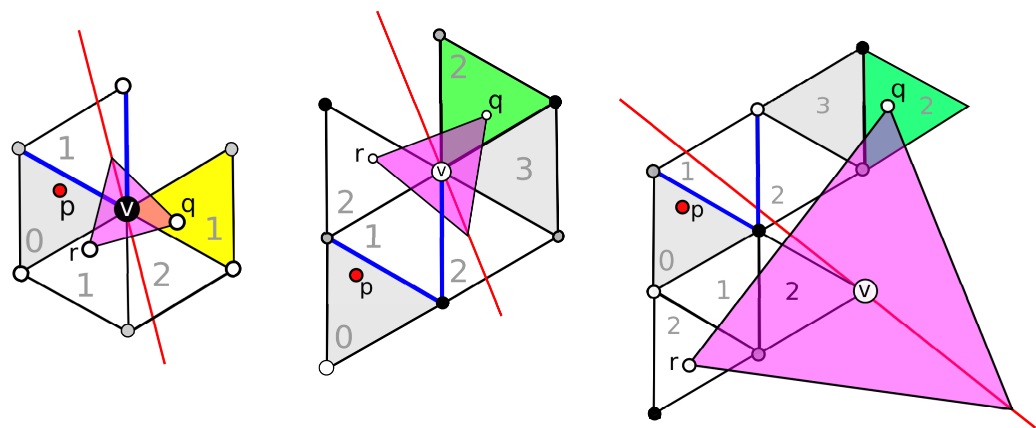

Figure 3.2: The three cases

The three cases have the same proof. Let τ be the equilateral triangle centered at the vertex v and having q as a vertex. Let r be the other shown vertex of τ. Note that all points of Δ_0 except perhaps for the sharp vertex (v on the left) lie on the same side of the bisector (r, q) as does r. Hence $|p - r| < |p - q|$. We get strict inequality because $q \not\in P$. We claim that $r^* = \Psi(r)$ and q^* lie in the same face. Assuming this claim, the positions of q and r in their respective faces with respect to the vertex coloring is the same. Hence $r^* = q^*$. But $\Psi(\overline{pr})$ has the same endpoints as α^* and is shorter. Contradiction.

Now for the claim. In the yellow case, we roll X one click counterclockwise about v to reach the face containing r and we roll X three clicks clockwise about v to reach q. Since the cone angle at v is 4 times the interior angle of a single equilateral triangle, we see that r^* and q^* lie in the same face. In the middle green case, the reason is essentially the same. For the righthand green case, let ζ be the face having 2 blue edges. Given the nature of α, we see that q lies in the face antipodal to $\Psi(\zeta)$. But r^* also lies in the face antipodal to $\Psi(\zeta)$. Hence r^* and q^* lie in the same face. ♠

3.2 Points in the Farthest Point Set

We revert to the original labeling of the octahedral plan, as in Figure 2.1. Suppose $q^* \in F_p$. Let q be as in Lemma 3.1. We suppose that q does not lie in a 7-face and we derive a contradiction. If q avoids all k faces for $k > 3$ then we can choose $s \in \overrightarrow{pq}$ such that $|p - s| > |p - q|$ and $\Psi^{-1}(s^*) = \{s\}$, where $s^* = \Psi(s)$. But then we have a contradiction:

$$d_X(p, q^*) = |p - q| < |p - s| = d_X(p, s^*).$$

The last equality is Lemma 3.1.

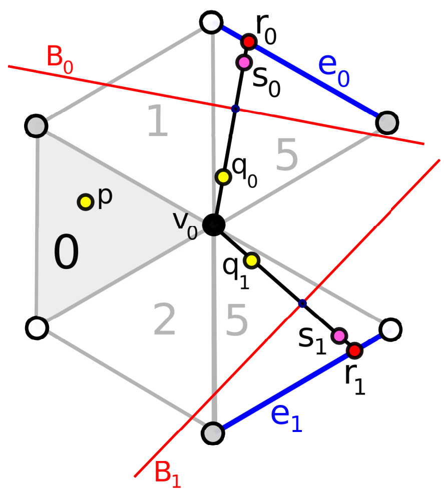

Figure 3.3: Pushing out q_j towards r_j.

For the remaining cases, we can assume by symmetry that q lies in a 5-face and avoids all 7-faces. Our argument refers to Figure 3.3. We have $q \in \Psi^{-1}(q^*) = \{q_0, q_1\}$ where q_j lies in the 5-face sharing an edge e_j with A_j. Let $r_j = e_j \cap \overleftrightarrow{v_0 q_j}$ (or else the midpoint of e_j when $v_0 = q_0 = q_1$.) Let B_j be the bisector defined by (q_j, r_j). The face Δ_0 lies on the same side of B_j as does q_j. Therefore $|p - r_j| > |p - q_j|$. Rotation by 120 degrees clockwise about v_0 maps (q_0, r_0, q_0) to (r_1, r_1, e_1).

By continuity and symmetry, there exists points $s_j \in \overline{q_j r_j}$ which avoid the 7-faces and satisfy $|p - s_j| > |p - q_j|$ and $s^* = \Psi(s_0) = \Psi(s_1)$. But then $\Psi^{-1}(s) = \{s_0, s_1\}$ and we have a contradiction:

$$d_X(p, q^*) = \min(|p - q_0|, |p - q_1|) < \min(|p - s_1|, |p - s_2|) = d_X(p, s^*).$$

The last equality is Lemma 3.1.

4 The Calculations

4.1 Structural Stability

We will be considering functions on T, the fundamental domain. It will be more convenient to deal with functions on the unit square $[0,1]^2$. So, we explain a convenient map from $[0,1]^2$ to T. We define

$$(x,y) = \phi(a,b) = \left(a + \frac{1}{4}(1-a)b, \frac{\sqrt{3}}{4}(1-a)b\right). \tag{15}$$

Here ϕ is a surjective polynomial map from $[0,1]^2$ to T which maps $(0,1)^2$ onto T^o. We get ϕ by composing the map $(a,b) \to (a,ab)$ with an affine map from the triangle with vertices $(0,0)$, $(1,0)$, $(1,1)$ to T.

We first prove the Structural Stability Lemma for $p \in T^o$. The combinatorics of the Voronoi decomposition can change only if one of the edges of the cell decomposition collapses to a point. The only edges for which this can happen are those joining consecutive points on the list (012), (025), (235), (345). Such an edge collapses if and only if one of the quadruples (0125), (0235), (2345) is such that the corresponding vertices are equidistant from a single point – i.e. co-circular. We rule this out.

As is well known, 4 distinct points $z_1, z_2, z_3, z_4 \in \boldsymbol{C}$ are co-circular if and only if

$$\chi(z_1,z_2,z_3,z_4) = \mathrm{Im}\Big((z_1-z_2)(z_3-z_4)\overline{(z_1-z_3)(z_2-z_4)}\Big) = 0. \tag{16}$$

This function is the imaginary part of the cross ratio. Thus, it suffices to prove that the 3 functions

$$T_{ijk\ell} = \frac{16}{27\sqrt{3}}\chi(p_i,p_j,p_k,p_\ell) \circ \phi, \tag{17}$$

corresponding to the quads above never vanish on $(0,1)^2$. The factor out in front is included to make the formulas below nicer. Now we give formulas for the vertices of H_p. Let

$$Z(k_1,\ell_1,k_2,\ell_2;p) = w(k_1,\ell_1)p + w(k_2,\ell_2), \qquad w(k,\ell) = \frac{k+\ell\sqrt{3}i}{2}. \tag{18}$$

We have $p = p_0 = x + iy$, and then a careful inspection of Figure 2.2 gives us

1. $p_1 = Z(-1, +1, +3, -1; p)$.
2. $p_2 = Z(-1, -1, +9, +1; p)$.
3. $p_3 = Z(+2, +0, +9, +3; p)$.
4. $p_4 = Z(-1, +1, +3, +5; p)$.
5. $p_5 = Z(-1, -1, +0, +4; p)$.

We plug this in to Equation 17 and factor using Mathematica [**Wo**]:

$$T_{0125} = (a-1)b\nu_1, \quad T_{2345} = (1-a)b\nu_2, \quad T_{0235} = 24a(a-1)(b-1). \tag{19}$$

Here, ν_1 and ν_2 are positive on $[0,1]^2$:

$$\nu_1 = (8 - 4a^2 - b^2) + (8a - 4ab - a^2b^2) + (2b + 2a^2b + 2ab^2)$$
$$\nu_2 = (16a - 2ab - 2a^2b - 2ab^2) + (4 + a^2b^2 + 4a^2 + 4b + b^2)$$

Hence our 3 functions in Equation 19 are positive on $(0,1)^2$. This completes the proof when $p \in T^o$.

For the boundary case, we just have to see that there is no $p \in \partial T$ such that the cells $C_{i_1}, ...C_{i_k}$ meet at a point and less than 3 of these indices come from one of the 4 triples above. If this happens, then by continuity the same thing happens when p is perturbed into T^o. Hence, this does not happen. This proves the Structural Stability Lemma in the boundary case.

Remark: The case when p lies in the interior of the bottom edge of T corresponds to $b = 0$ and $a \in (0,1)$. In this case, $T_{0235} \neq 0$. This means that (012) and (235) are distinct in this case.

4.2 The Vertex Competition

In this section we calculate the function G from §2.5. Using the formulas for the vertices listed above, we compute the relevant bisectors and the relevant intersections of these bisectors to arrive at formulas for the essential vertices. Here they are.

$$(012) = \frac{3\sqrt{3}x^2-6yx-11\sqrt{3}x+21y+5y^2\sqrt{3}+8\sqrt{3}}{2\left(\sqrt{3}x^2-3\sqrt{3}x+3y+y^2\sqrt{3}+2\sqrt{3}\right)} + i\,\frac{3x^2-2\sqrt{3}yx-15x-3y^2-\sqrt{3}y+12}{2\left(\sqrt{3}x^2-3\sqrt{3}x+3y+y^2\sqrt{3}+2\sqrt{3}\right)}$$

$$(025) = \frac{2\sqrt{3}y^2+2xy-3y+3x\sqrt{3}-8\sqrt{3}}{2\left(y+x\sqrt{3}-2\sqrt{3}\right)} + i\,\frac{2y^2-2\sqrt{3}xy+3\sqrt{3}y+3x-12}{2\left(y+x\sqrt{3}-2\sqrt{3}\right)}$$

$$(235) = \frac{\sqrt{3}y^2+xy+3y+3x\sqrt{3}+2\sqrt{3}}{y+x\sqrt{3}+\sqrt{3}} + i\,\frac{y^2-\sqrt{3}xy+6x+3}{y+x\sqrt{3}+\sqrt{3}}$$

$$(345) = \frac{3\sqrt{3}x^2+8\sqrt{3}x-3y+y^2\sqrt{3}+4\sqrt{3}}{\sqrt{3}x^2+3\sqrt{3}x-3y+y^2\sqrt{3}+2\sqrt{3}} + i\,\frac{6x^2+2y\sqrt{3}x+15x+6y^2-2\sqrt{3}y+6}{\sqrt{3}x^2+3\sqrt{3}x-3y+y^2\sqrt{3}+2\sqrt{3}}$$

For G we don't make the change of variables, but rather compute in terms of $p = x + iy \in T^o$. We have

$$G = -\frac{18H}{\left(\sqrt{3}x + y - 2\sqrt{3}\right)^2 \left(\sqrt{3}x + y + \sqrt{3}\right)^2},$$

where

$$H = \begin{pmatrix} 3x^5 - 6x^4 - 9x^3 + 15x^2 - 3x \\ 3\sqrt{3}x^4 - 4\sqrt{3}x^3 - 6\sqrt{3}x^2 - 3\sqrt{3}x + \sqrt{3} \\ 2x^3 - 6x^2 + 15x - 2 \\ 2\sqrt{3}x^2 - 2\sqrt{3} \\ -x + 4 \\ -\sqrt{3} \end{pmatrix} \cdot \begin{pmatrix} 1 \\ y \\ y^2 \\ y^3 \\ y^4 \\ y^5 \end{pmatrix}$$

The denominator is positive on T, so the sign of H determines the sign of the whole expression. Using Mathematica to solve the equation $H = 0$ for y in terms of x, we find that the solutions are

$$y = \frac{x-1}{\sqrt{3}}, \qquad y = \sqrt{3}x,$$

$$y = \frac{1}{\sqrt{3}}\left(1 - x - \omega^k((2+x)(5-2x)(1-4x))^{1/3}\right). \tag{20}$$

Here $\omega = \exp(2\pi i/3)$ and $k = 0, 1, 2$. The first two solutions correspond to the sides of $\partial_\infty(T)$. This third solution intersects T only when $k = 0$. This is precisely the function in Equation 4, the one which defines the curve J from the Main Theorem. Finally, $G(1/2, 0) = -1/3$, which shows that G is positive to the left of J and negative to the right, when restricted to $T - \partial_\infty T$. This establishes everything we needed to know about G.

5 References

[**MP**] E. Miller and I. Pak, *Metric Combinatorics of Convex Polyhedra: Cut Loci and Nonoverlapping Foldings*, arXiv:math/0312253v1 (2003)

[**R1**] J. Rouyer, *Antipodes sur le tétraèdra régulier*, J. Geom. **77** (2003), no. 4, pp. 152-170.

[**R2**] J. Rouyer, *On antipodes on a convex polyhedron*, Adv. Geom. 5 (2005), no. 4, pp. 497-507.

[**R3**] J. Rouyer, *On antipodes on a convex polyhedron II* , Adv. Geom. 10 (2010), no. 3, pp. 403-417.

[**S1**] R. E. Schwartz, *Spiders Embrace*, Java graphical interface (2015, updated 2020), download from
http://www.math.brown.edu/∼res/Java/Spider.TAR.

[**V1**] C. Vılcu, *On two conjectures of Steinhaus*, Geom. Dedicata 79 (2000), no. 3, pp 267-275.

[**V2**] C. Vılcu, *Properties of the farthest point mapping on convex surfaces*, Rev. Roum. Math. Pures Appl. 51 (2006), no. 1, 125-134.

[**VZ**] C. Vılcu and T. Zamfirescu, *Multiple farthest points on Alexandrov surfaces*, Adv. Geom. 7 (2007), no. 1, pp 83-100.

[**W**] Z. Wang, *Farthest Point Map on a Centrally Symmetric Convex Polyhedron*, Geometriae Dedicata **204** (2020) pp 73-97.

[**Wo**] S. Wolfram, *Mathematica* (2020) wolfram.com/mathematica

[**Z**] T. Zamfirescu, Extreme points of the distance function on a convex surface, Trans. Amer.Math.Soc. 350(1998), no. 4, 1395-1406.